STR🌀BE-X

STROBE-X: X-ray Timing and Spectroscopy on Dynamical Timescales from Microseconds to Years

A Probe Class Mission Concept APC White Paper
Submitted to Astro 2020 Decadal Survey

Paul S. Ray
U.S. Naval Research Laboratory
`paul.ray@nrl.navy.mil`

***STROBE-X* Steering Committee:** Zaven Arzoumanian, David Ballantyne, Enrico Bozzo, Soren Brandt, Laura Brenneman, Deepto Chakrabarty, Marc Christophersen, Alessandra DeRosa, Marco Feroci, Keith Gendreau, Adam Goldstein, Dieter H. Hartmann, Margarita Hernanz, Peter Jenke, Erin Kara, Tom Maccarone, Michael McDonald, Michael Nowak, Bernard Phlips, Ron Remillard, Abbie Stevens, John Tomsick, Anna Watts, Colleen Wilson-Hodge, Kent Wood, Silvia Zane

***STROBE-X* Science Working Group:** Marco Ajello, Will Alston, Diego Altamirano, Vallia Antoniou, Kavitha Arur, Dominic Ashton, Katie Auchettl, Tom Ayres, Matteo Bachetti, Mislav Baloković, Matthew Baring, Altan Baykal, Mitch Begelman, Narayana Bhat, Slavko Bogdanov, Michael Briggs, Esra Bulbul, Petrus Bult, Eric Burns, Ed Cackett, Riccardo Campana, Amir Caspi, Yuri Cavecchi, Jerome Chenevez, Mike Cherry, Robin Corbet, Michael Corcoran, Alessandra Corsi, Nathalie Degenaar, Jeremy Drake, Steve Eikenberry, Teruaki Enoto, Chris Fragile, Felix Fuerst, Poshak Gandhi, Javier Garcia, Adam Goldstein, Anthony Gonzalez, Brian Grefenstette, Victoria Grinberg, Bruce Grossan, Sebastien Guillot, Tolga Guver, Daryl Haggard, Craig Heinke, Sebastian Heinz, Paul Hemphill, Jeroen Homan, Michelle Hui, Daniela Huppenkothen, Adam Ingram, Jimmy Irwin, Gaurava Jaisawal, Amruta Jaodand, Emrah Kalemci, David Kaplan, Laurens Keek, Jamie Kennea, Matthew Kerr, Michiel van der Klis, Daniel Kocevski, Mike Koss, Adam Kowalski, Dong Lai, Fred Lamb, Silas Laycock, Joseph Lazio, Davide Lazzati, Dana Longcope, Michael Loewenstein, Renee Ludlam, Dipankar Maitra, Walid Majid, W. Peter Maksym, Christian Malacaria, Raffaella Margutti, Adrian Martindale, Ian McHardy, Manuel Meyer, Matt Middleton, Jon Miller, Cole Miller, Sara Motta, Joey Neilsen, Tommy Nelson, Scott Noble, Paul O'Brien, Julian Osborne, Feryal Ozel, Nipuni Palliyaguru, Dheeraj Pasham, Alessandro Patruno, Vero Pelassa, Maria Petropoulou, Maura Pilia, Martin Pohl, David Pooley, Chanda Prescod-Weinstein, Dimitrios Psaltis, Geert Raaijmakers, Chris Reynolds, Thomas E. Riley, Greg Salvesen, Andrea Santangelo, Simone Scaringi, Stephane Schanne, Jeremy Schnittman, David Smith, Krista Lynne Smith, Bradford Snios, Andrew Steiner, Jack Steiner, Luigi Stella, Tod Strohmayer, Ming Sun, Thomas Tauris, Corbin Taylor, Aaron Tohuvavohu, Andrea Vacchi, Georgios Vasilopoulos, Alexandra Veledina, Jonelle Walsh, Nevin Weinberg, Dan Wilkins, Richard Willingale, Joern Wilms, Lisa Winter, Michael Wolff, Jean in 't Zand, Andreas Zezas, Bing Zhang, Abdu Zoghbi

1 Introduction

STROBE-X is a probe-class (\$0.5–1B) mission concept, selected for study by NASA, for X-ray spectral timing of compact objects across the mass scale. It combines huge collecting area, high X-ray throughput, broad energy coverage, and excellent spectral and temporal resolution in a single facility. The mission carries three instruments: the 0.2–12 keV X-ray Concentrator Array (XRCA), the 2–30 keV Large Area Detector (LAD), and the 2–50 keV Wide-Field Monitor (WFM). All are based on demonstrated technology: XRCA scales up from a small modification of the flight-proven optics and detectors from *NICER*, while LAD and WFM are based on large-area silicon drift detectors previously developed for the ALICE/LHC high-energy physics experiment at CERN.

Through advances in silicon detector and microchannel plate collimator technologies over the past two decades, *STROBE-X* delivers an order-of-magnitude increase in sensitivity relative to previous missions. In the soft X-ray band, its collecting area is $20\times$ larger than *XMM*/pn and $10\times$ larger than *NICER*. In the hard X-ray band, it has superior spectral resolution and 9 times the area of *RXTE*, which had the equivalent of a probe-class budget in the 1990s. Crucially, *STROBE-X* provides $25\times$ the area in the 6–7 keV Fe Kα line region as future missions *Athena* and *Lynx*, making it far more sensitive to variability of this key diagnostic line. These advances greatly increase the power of X-ray spectral timing techniques for Galactic sources and extend their reach to extragalactic targets for the first time. *STROBE-X* is also an agile mission capable of rapid response to transient events, making it an essential X-ray partner facility in the era of time-domain, multi-wavelength and multi-messenger astronomy.

As requested in the APC call, this document is a self-contained, condensed version of the full 50-page *STROBE-X* study report submitted to NASA, which is available at arXiv:1903.03035.

2 Key Science Goals and Objectives

STROBE-X is optimized for the study of the most extreme conditions in the Universe and has several key science objectives, including: (1) Robustly measuring spin and mapping inner accretion flows across the black hole mass spectrum, from compact stars to intermediate-mass objects to active galactic nuclei; (2) Mapping out the full mass-radius relation of neutron stars, using an ensemble of 20 rotation-powered pulsars and accreting neutron stars, and hence measuring the equation of state of ultradense matter over a much wider range of densities than can be explored by *NICER* or LIGO; (3) Identifying and studying X-ray counterparts in the post-*Swift* era, for multiwavelength and multi-messenger transients in the dynamic sky through cross-correlation with gravitational wave interferometers, neutrino observatories, and high-cadence time-domain surveys in other electromagnetic bands; and (4) Continuously surveying the dynamic X-ray sky with a large duty cycle and high time resolution to characterize the behavior of X-ray sources over an unprecedentedly vast range of time scales. The mission's formidable capabilities will also enable a broad portfolio of additional science including the study of accretion physics, stellar evolution, stellar flares, gamma-ray bursts, tidal disruption events, active galactic nuclei, clusters of galaxies, and axion searches.

Black Hole Spins. Understanding black hole spins is important both as a test of general relativity [7] and as a probe of the formation and evolution of black holes [14, 29]. Especially in the era of gravitational wave estimates of black hole spin (which have their own systematic uncertainties)[47], electromagnetic spin measurements are vital, as they are sensitive to different evolutionary channels for stellar mass black holes. For supermassive black holes, single objects can be studied, rather than just binaries, and the heaviest objects can be studied rather than just the $< 10^7 M_\odot$ black holes that LISA can detect.

For stellar-mass black holes in "soft" spectral states, the X-ray spectra are very well modeled by standard accretion disk models where the emission in each annulus is a diluted blackbody with
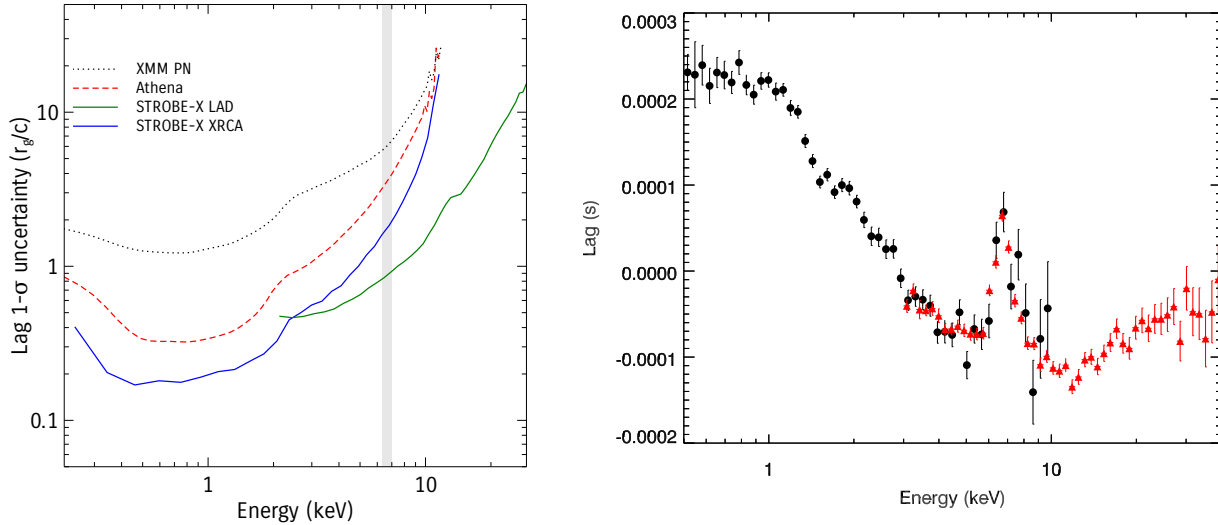
Figure 1: *STROBE-X* is the most sensitive mission for reverberation mapping across its entire bandpass. Left: *STROBE-X* (solid curves) compared with other satellites (dotted curves) for an AGN black hole, assuming a 2 mCrab source, 100 ks exposure, and a $10^6 M_\odot$ black hole. The Fe-K line region near 6.4 keV is denoted by the grey band. Right: A simulated 1 ks *STROBE-X* observation of the XRB black hole GX 339-4 showing 1–10 Hz reverberation lags (XRCA shown as black circles, LAD as red triangles), with parameters following those of Ref. 44. The LAD lag precision at the Fe-K line is about 20 μs per spectral bin in a 1 ks observation, significantly better than 1 R_g/c (a gravitational radius crossing time) for a 10 $M_\odot$ black hole.

its temperature set by the gravitational energy release from matter falling through that annulus [40, 42]. For any given source, the model-fit radius is constant over repeated measurements at different accretion rates [10]. The inner disk radius in Schwarzschild units does vary substantially from source to source. Studying a range of cases provides good evidence that it is likely that the inner radius is to be identified with the innermost circular orbit around the black hole and, from that, that black holes have a range of spin values[10]. The physics of this method is best understood, but application relies on knowing the distance and mass of the black hole and the inclination angle of the accretion disk.

Reflection spectroscopy is generally applied in spectral states with more hard X-ray emission than the disk fitting method. The spectrum of the accretion disk results from the effects of illumination from the hard X-rays. This spectrum is given by a sum of relativistically-broadened absorption edges and emission lines (with fluorescent Fe Kα at 6.4–6.7 keV being the strongest), reprocessed thermal emission driven by the external heating (in the 0.1–2.0 keV range) and a Compton reflection hump (peaking at about 30 keV), taking account of both Doppler boosts and gravitational redshifts [15, 51]. The emission line profiles are independent of black hole mass and distance, and the effects of the inclination angle are so strong that they can be measured directly. The models contain uncertainty about the geometry of the corona. Currently, this issue is typically handled by making assumptions, but it has recently been established that measurement of time lags between different energy bands due to light travel times (so-called X-ray reverberation mapping) can resolve these uncertainties [43].

STROBE-X will provide exquisite reflection spectra for both stellar-mass black holes and a large number of supermassive black holes. Simulations have shown that for spectral resolution better than about 500 eV, greater collecting area does more to improve precision of measurements than greater spectral resolution [37]. Only *STROBE-X* has the effective area to make the reverberation mapping measurements for stellar mass black holes which, while brighter than supermassive black

holes, have lower count rates per light crossing timescale than the supermassive black holes [37] – see Fig. 1. More speculatively, high-frequency quasi-periodic oscillations provide very precise measurements which are very likely to be tied to the black hole spin due to their frequencies exceeding those of Keplerian orbits around non-rotating black holes. With *STROBE-X*, both the detection of higher modes of these oscillations and measurements of emission line variations in these modes will break model degeneracies and provide a potential independent mechanism for precision spin measurements [37, 42].

STROBE-X will thus make about 20 black hole spin measurements each for supermassive and stellar mass black holes [37], but, perhaps more importantly, it is the only proposed mission capable of testing the different approaches for measuring spins against one another. While future missions like *Athena* and *Lynx*, with their superior angular resolution, can make measurements of reflection spectra for AGN fainter than those *STROBE-X* can observe, only with *STROBE-X*'s multi-pronged approach to studying the X-ray binaries and the brightest AGN, can the reflection spectroscopy approach be refined so that it can then be applied to systems without cross-checks available. Furthermore, *STROBE-X*'s flexible scheduling will enable it to make multiple measurements using each method for each source, allowing checks for internal consistency of the methods.

Equation of State of Ultradense Matter.   The mass-radius relationship of neutron stars maps directly to the pressure-density relationship for supranuclear-density material. Understanding the equation of state of ultradense matter gives unique constraints on high-energy physics that are not accessible from particle accelerators. The equation of state of ultradense matter can be approached from a variety of methods. Pulsar timing and radial velocity curve measurement of binary neutron stars can be used to search for the most massive neutron stars (which can rule out some equations of state), but cannot be used to estimate neutron star radii. Radio pulsar timing of relativistic binaries can in principle deliver radii via moment of inertia measurements, and at least one such measurement is anticipated from the Double Pulsar, but getting more measurements relies on new sources being identified [25]. Gravitational waves from NS-NS or NS-BH mergers will deliver constraints on masses and tidal deformabilities, but a few tens of detections are needed in order to make few percent level estimates, and incomplete waveform modeling and non-rigid body rotation of the neutron stars are likely to yield systematic errors of the same order [38]. Furthermore, the strong evidence for massive neutron stars to date puts all of them in binaries with low mass companions. It is likely that these systems have grown substantially by accretion, which can happen only in the long-lived low mass X-ray binaries that are the progenitors of millisecond pulsars, but which cannot become double neutron star systems. LIGO and double pulsars are thus unlikely to sample the massive end of the neutron star distribution. X-ray measurements thus remain vital for obtaining high precision masses and radii [4].

STROBE-X has multiple approaches available for understanding the equation of state of neutron stars through pulse profile modeling [2]. The shape and the spectrum of the pulses yield information about the radii (through doppler shifts) and the ratio of mass to radius (through gravitational redshifts and light bending). Measurements can be made for rotation-powered pulsars, accretion-powered pulsars and Type I X-ray burst oscillations with *STROBE-X*. About 10^6 photons are needed to obtain good pulse profiles [37, 4, 13]. Pulse profile modelling does depend on assumptions about e.g. hotspot morphology, but Bayesian model comparison (e.g. looking for residuals between data and model, and computation of evidences) allows us to identify the preferred configuration. *NICER* will be able to apply this method for 4 objects, but *STROBE-X*'s collecting area is needed to make good measurements of about 20 neutron stars in order to span a broad range of masses. *STROBE-X* is also ideal for complementary, albeit more speculative, approaches to measuring M/R, like searches for photospheric absorption lines during Type I X-ray bursts [4]. Fig. 2 illustrates what *STROBE-X* can be expected to do for the equation of state.
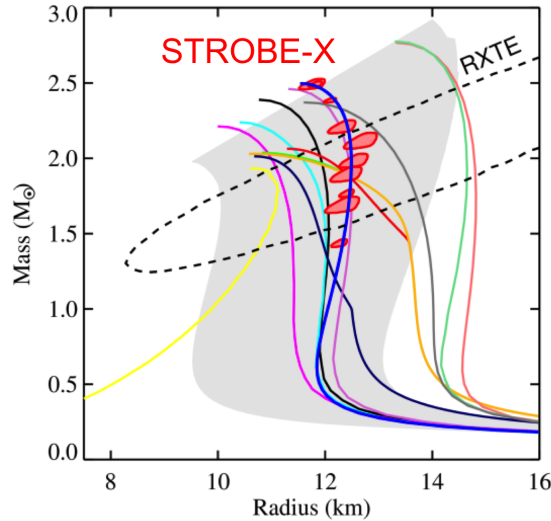
Figure 2: *STROBE-X* will tightly constrain the equation of state using ~ 20 neutron stars. The red ellipses illustrate how 5% measurements of M and R from many neutron stars, as expected from *STROBE-X*, will map out the full M-R relation and thus tightly constrain the ultradense matter equation of state (EOS). The current *NICER* mission will only measure ~ 4 neutron stars. An earlier *RXTE* constraint is also shown. The M-R curve for the "true" EOS (blue in this example) must be consistent with all observations. The other colored curves are M-R relations for other representative EOS models [27], and the grey band shows the range of EOS models based on chiral effective field theory [20].

Multimessenger Astrophysics *STROBE-X* has a multi-pronged approach for multi-messenger astronomy, with strengths geared not just to the problems facing us today, but also to the discovery space likely to emerge in a new era with upgraded gravitational wave detectors. The *STROBE-X* WFM will have excellent sensitivity to a wide range of gamma-ray bursts (GRBs), including nearby off-axis short gamma-ray bursts (the high energy counterparts to merging neutron stars), and to blazars (which will be monitored to provide information about potential neutrino counterparts). [37, 39]. The WFM can also detect shock breakouts from supernovae within 20 Mpc (meaning the horizon distance for *STROBE-X* and *LIGO* in the 2030s should be similar for core collapse supernovae) [37, 21]. Its instantaneous field of view of 1/3 of the sky will yield a high detection rate of these events, and its 1 arcmin positional accuracy (about 10 times better than SVOM's) is suitable for spectroscopic follow-up of bright transients (whether supernova shock breakouts or short GRBs) with integral field units without further follow-up. The high throughput pointed instruments allow follow-up of future continuous sources of gravitational waves, both rotation and accretion-powered pulsars [21, 41] that should emit gravitational waves in the LIGO band, and pulsars in ultracompact binaries that should emit gravitational waves in the LISA band [26]. With sufficient sensitivity, X-ray searches for pulsars can become more complete than radio searches because X-ray pulse beam opening angles are typically larger than radio opening angles. The *STROBE-X*/XRCA can be used to make timing measurements of millisecond pulsars deep in the Galactic Plane for which dispersion and scattering make radio timing difficult, meaning that *STROBE-X* can play an important niche role in the Pulsar Timing Array [9]. All-sky monitoring in the hard X-rays can detect merging quasars' quasi-periodic oscillations [24].

A Broad Astrophysics Portfolio While *STROBE-X*'s design is optimized for the three key science goals above, it has huge potential for major contributions across the broad range of astrophysics from solar system studies to cosmology. In total, 15 of the Astro2020 science white papers explicitly mention *STROBE-X*, while at least 58 white papers discussed topics to which *STROBE-*

X could make a major contribution, and 25 more were topics for which *STROBE-X* could play a supporting role. Half of these papers were on the key science goals above, and half were on the broader astrophysics studies that could be done with *STROBE-X*. They outline connections between *STROBE-X* and LIGO, LISA, LSST, large optical telescopes, the Next Generation Very Large Array, and the Square Kilometer Array, neutrino facilities, and high energy gamma-ray facilities. It also connects strongly to the nuclear physics community, both through equation of state measurements, and studies of Type I X-ray bursts, the nuclear reactions in which were one of the core motivations for the construction of the National Superconducting Cyclotron Laboratory [32].

Accretion Physics — *STROBE-X* will study the dynamics of accretion flows on the most rapid timescales [42, 22], including ultraluminous and ordinary accreting pulsars [6, 48], the rapid variability of disk winds and the coupling of relativistic jets to the disks that power them [42, 29], and hence will allow studies of extrema of plasma physics [45]. It will discover tens of jetted tidal disruption events per year, while making follow-up observations of both jetted and non-jetted events [23, 37]. It will monitor both ordinary AGN, providing power spectra which can be used to estimate their masses [31], with sensitivity to thousands of AGN, including the brightest quasars out to $z \sim 2$ [37]; and blazars, enhancing the ability to interpret their high-energy gamma-rays. *STROBE-X* is also capable of light echo monitoring of the Galactic Center region, providing new insights about the past accretion history of our own galaxy's supermassive black hole [18].

Stellar Evolution — *STROBE-X* will produce new discoveries of X-ray binaries to help expand their populations so that the formation of black holes and neutron stars in supernovae can be probed [30], while also providing the capability to use X-ray spectroscopy to classify supernova remnants [37, 50]. For low-mass stars, *STROBE-X*/WFM will detect the most extreme stellar flares [37, 11], and be able to make high-quality spectra and light curves of them through automated re-pointing of *STROBE-X*/XRCA [37], allowing both the physics and the rates of these events to be studied [34], while also providing an external trigger for low frequency radio searches for exo-aurorae [28].

Extragalactic Astronomy — *STROBE-X* will allow measurements of chemical abundances in galaxy groups, and on the outskirts of galaxy clusters [37]. The full-sky survey from the *STROBE-X*/WFM will be by far the deepest ever made in medium-energy X-rays, and should have Fe Kα line-based searches for low-redshift, Compton-thick AGN significantly more sensitive than *eROSITA*'s continuum survey [1, 8]. It provides unique sensitivity to two methods for searching for axions, through enhanced cooling of neutron stars, and through "wiggles" in the spectra of AGN in clusters of galaxies [19, 37]. The medium-energy X-ray coverage of the *STROBE-X*/WFM is ideal for finding high-z GRBs.

3   Technical Overview

STROBE-X comprises three instruments, each with a critical role to play. The technical designs are described in detail by Ray et al. [36] and Ray et al. [37]. Our primary science goals drive the instrument and mission requirements, but the mission will be capable of performing a broad program of astrophysics that will be implemented through a vibrant guest observer program.

The primary instruments are both single-pixel instruments with collecting areas an order of magnitude larger than previous missions, with high time resolution and good spectral resolution recorded for every detected photon. Combined, the two instruments cover the range 0.2–30 keV, with substantial overlap such that both instruments are highly capable around the critical iron line region. The low-energy instrument has lower background (due to its concentrating optics), which gives it superb sensitivity to faint thermal sources and it has better spectral resolution that allows studies of atomic lines and edges in the soft X-ray band. The high-energy instrument has larger collecting area, optimized for time-domain studies of Comptonization and reflection components and rapid hard X-ray variability. These are complemented by a wide field monitor that provides transient source localization, source spectral state characterization, and an X-ray all-sky survey

and monitoring capability.

The team has created detailed designs, driven by science requirements, and prepared thorough cost estimates during a study at the NASA/GSFC Instrument Design Lab (IDL) in 2017 November and December. A key result of this study was the division of the primary instrument into four identical "quadrants," each with a composite optical bench and a deployable panel. This design has several advantages. First, integration and test flow are simplified. Testing can incorporate parallelism and is thereby reduced in cost. It furthermore requires smaller facilities than if the instruments were a monolithic unit. Second, system reliability is improved because of the modularity that allows any one quadrant to fail without bringing the observatory capabilities below the science requirements. Finally, the composite optical bench has reduced mass, increased stiffness, and a reduced coefficient of thermal expansion relative to earlier aluminum structural designs. We give only a brief description of each instrument here.
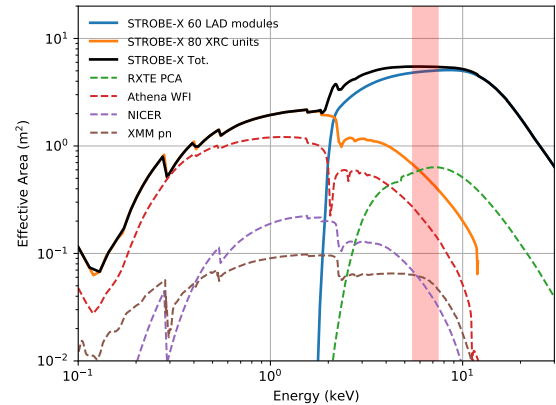

Figure 3: Effective area of the *STROBE-X* pointed instruments (solid curves), compared to some previous and planned missions (dashed curves). *STROBE-X* has the largest area over its entire bandpass. The Fe-K line region is shown by the pink band.

X-ray Concentrator Array (XRCA). *STROBE-X* covers the soft X-ray (0.2–12 keV) band with the XRCA instrument, a modular collection of identical X-ray "concentrator" (XRC) units that leverage the successful design and development efforts associated with GSFC's X-ray Advanced Concepts Testbed (*XACT*) sounding-rocket payload [3] and the *NICER* mission [17, 33].

Concentration is accomplished with single parabolic grazing-incidence optics, instead of the multi-mirror configurations needed for imaging performance. This enables several key efficiencies and cost savings: 1) X-rays only suffer reflection inefficiencies once, resulting in enhanced effective area; 2) the number of optical elements required is half that of an imaging configuration, resulting in substantial cost and schedule savings; and 3) with no need to align primary and secondary optics, integration is significantly simplified.

The detectors are the same commercially-available silicon drift detectors (SDDs) that were used for *NICER*. Built-in thermoelectric coolers (TECs) maintain a constant detector temperature of $-55°$ C. The performance parameters of the XRCA instrument are shown in Fig. 1.

Large Area Detector (LAD). The LAD is a large-area, collimated instrument, operating in the 2–30 keV nominal energy range. The concept and design of the LAD instrument is based on the same instrument proposed as part of the scientific payload of the ESA *LOFT* mission concept [12, 49]. The design of such a large instrument is feasible thanks to the detector technology of the large-area SDDs [16], developed for the ALICE/LHC experiment at CERN [46] and later optimized for the detection of photons for X-ray astronomy missions [35], with typical size of 11×7 cm^2 and 450 μm thickness. The key properties of the SDDs are their capability to read out a large photon collecting area with a small set of low-capacitance (thus low-noise) anodes and their very low mass ($\sim$1 kg m^{-2}).

Taking full advantage of the compact detector design requires a similarly compact collimator design. This is provided by the capillary plate technology. In the LAD geometry, the capillary plate is a 5 mm thick sheet of lead-glass (>40% Pb mass fraction) with the same size as the SDD detector, with round micro-pores 83 μm in diameter, limiting the field of view (FoV) to 0.95° (full
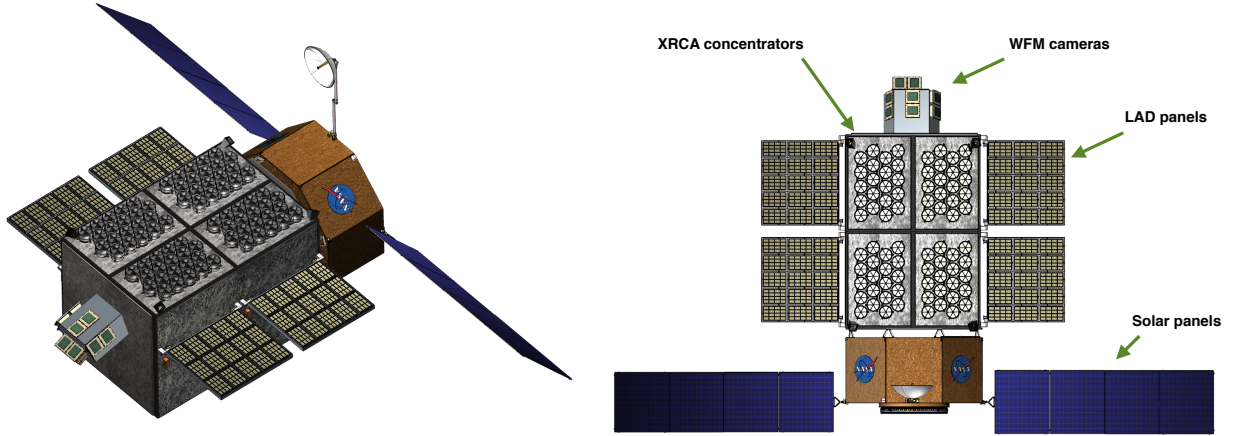
Figure 4: Detailed design renderings of the *STROBE-X* mission from the NASA/GSFC Instrument Design Laboratory (IDL) and Mission Design Laboratory (MDL).

width at half maximum). The open area ratio of the device is 75%.

Wide-Field Monitor (WFM). The WFM is a coded mask instrument consisting of four pairs of identical cameras, with position-sensitive detectors in the 2–50 keV energy range. The same SDDs as the LAD are used, with a modified geometry to get better spatial resolution. These detectors provide accurate positions in one direction but only coarse positional information in the other one (1.5D). Pairs of two orthogonal cameras are used to obtain precise two-dimensional (2D) source positions. The concept and design is inherited from the *LOFT* WFM instrument [12, 5].

The effective FoV of each camera pair is about $70° \times 70°$ ($30° \times 30°$ fully illuminated, $90° \times 90°$ at zero response). A set of four camera pairs is foreseen, with three pairs forming an arc covering $180°$ along the the sky band accessible to the LAD and XRCA, and the fourth pair aimed to monitor the anti-Sun direction. The parameters of the WFM are displayed in Fig. 2.

Mission Design. The overall mission concept, as developed in our GSFC Mission Design Lab (MDL) design, is that of an agile X-ray observatory in low-Earth orbit, similar to previous missions like *RXTE* and *Swift*. The spacecraft will launch on a Falcon 9 from KSC to a 550 km circular orbit, with orbital inclination as low possible. The launch capacity is 5130 kg to $10°$ inclination and 7730 kg to $15°$. We have included a capable propulsion system in the design for reboosting to increase orbital lifetime, debris avoidance maneuvers, and eventual safe disposal.

STROBE-X must be able to slew rapidly over the full sky outside of the $45°$ Sun avoidance region in order to follow transients, make monitoring observations, and respond rapidly to targets of opportunity. This $15°$/min slew rate goal can be met with high-TRL Honeywell control moment gyroscopes (CMGs). Attitude knowledge is provided by star trackers and coarse Sun sensors, and momentum unloading is accomplished with magnetic torquers.

An important feature is the downlink of all event data from the three instruments, removing the need for data modes that sacrifice spectral or time resolution for bright sources. We use TDRSS Ka-band downlink via a high gain antenna to achieve 300 Mbps, enabling downlink of 540 Gb/day on average. In addition, TDRSS S-band Multiple Access through a pair of omnidirectional antennas allows broadcasting of burst and transient alerts to the ground in less than 10 seconds as well as rapid commanding from the ground in response to a TOO request. The burst and transient alerts will be rapidly followed by localizations and quick look light curves, similar to *Swift* and *Fermi*/GBM.

Table 1: Expected Performance for the LAD and XRCA instruments

Large Area Detector (LAD)	
Number of Modules	60
Eff. Area per Module (cm^2)	850
Effective Area (cm^2 @ 10 keV)	51,000
Energy Range	2–30 keV
Detector	SDD (segmented large-area)
Background Rate (mcrab)	5
Background Rate (c/s)	822
Energy Resolution	200 – 300 eV FWHM
Collimator	1° FWHM
Time Resolution	10 µs
Count Rate on Crab (2-30 keV)	156,000
Telem Rate on 100 mcrab (kbps)	212

X-ray Concentrator Array (XRCA)	
Number of XRC units	80
Eff. Area per XRCU	272
Effective Area (cm^2 @ 1.5 keV)	21,760
Energy Range	0.2–12 keV
Detector	SDD (single pixel)
Background Rate (c/s)	2.2
Energy Resolution	85 – 175 eV FWHM
Collimator	4 arcmin FWHM
Time Resolution	100 ns
Count Rate on Crab (0.2-10 keV)	147,920
Bits per event, raw	70
Telem Rate on 100 mcrab (kbps)	597

Table 2: Expected Performance for the WFM instrument and the overall *STROBE-X* Mission

Wide-Field Monitor (WFM)	
# of Camera Pairs	4
FOV/Camera Pair	70° × 70° FWHM
Eff. Area/Camera Pair	364 cm^2
Optics	1.5-D coded mask
Energy Range	2-50 keV
Energy Resolution	300 eV FWHM
Detector	SDD (1.5D)
Sensitivity (1 s)	600 mcrab
Sensitivity (1 day)	2 mcrab
Sky Coverage (sr)	4.12
Angular Resolution	4.3 arcmin
Position Accuracy	1 arcmin
Telemetry Rate (kpbs)	140

STROBE-X Mission	
Instrument Mass (kg)	2,706
Spacecraft Bus Mass (kg)	1,737
Propellant (kg)	555
Total Mass (kg)	4,998
Orbit	LEO, 550 km altitude
Launcher	Falcon 9 FT
Launcher Capacity to LEO (kg)	5130 kg to 10° inclination
Instrument Power (W)	1,918
Spacecraft Power (W)	1,223
Attitude Control	3-axis stabilized, slew 15°/min
Solar Avoidance	< 45 deg
Data Gen/Orbit (raw, Gb)	36.0
Duration	5+ years

4   Technology Drivers

STROBE-X makes use of significant technology advancements compared to previous large-area X-ray missions that relied on massive and fragile gas detectors. Solid-state SDDs, coupled to microchannel plate collimators or lightweight aluminum concentrators, enable an order-of-magnitude improvement in collecting area with similarly improved energy resolution and with timing. These have all already been developed and most already have flight heritage on smaller instruments.

No new technologies are required to execute *STROBE-X*. However, some investment in raising the technology readiness level of the instruments would greatly increase the fidelity of the cost estimates, and would save money by shortening the development schedule. This can be done with a small number of APRA/SAT-scale programs.

The *STROBE-X* design makes use of many components with flight heritage, and the technology readiness level for the parts that have not yet flown is already quite high, as we describe here.

The XRCA instrument is directly based on the currently flying *NICER* instrument on the ISS. The biggest differences are the larger concentrators and the composite optical bench. Larger concentrators have already been built for the *XACT* sounding rocket payload and thus are at TRL 6, while the composite optical bench structure is new, but many similar composite structures are

in use (e.g. on *Fermi*, *SDO*, *LRO*).

The LAD design is directly inherited from the *LOFT* 3-year assessment study within the ESA M3 context. The experiment is based on two mature technologies: 1) large-area SDDs, with strong heritage in the Inner Tracking System of the ALICE/LHC at CERN, in which 1.4 m^2 of SDD with approximately the same design have been successfully operating since 2008; 2) the capillary plate collimators, similar to microchannel plates that have been successfully flown on several space missions in the past decades, including *Chandra*.

The WFM design is a conventional coded mask experiment but with the enhanced performance and low resources enabled by the same SDD as the LAD. A very similar design has been operating onboard the *AGILE* mission since 2007.

The spacecraft design from the MDL uses only TRL 7–9 components.

5   Organization, Partnerships, and Current Status

The *STROBE-X* study team is an experienced group combining people and institutions that have had leading roles in *NICER*, *LOFT*, and *Fermi*. We have worked closely together throughout the *LOFT* Assessment Phase study and now bring together the technologies and designs developed for *LOFT* with the flight-proven instruments from *NICER* into a combined mission that is more than the sum of its parts. *STROBE-X* has completed its funded concept study and is working towards having all components at high TRL in preparation for NASA implementing a probe-class mission line. It is important to note that while we have worked closely with our European partners throughout the study, we have done all budget estimates with the highly conservative assumption that NASA will fund 100% of the mission.
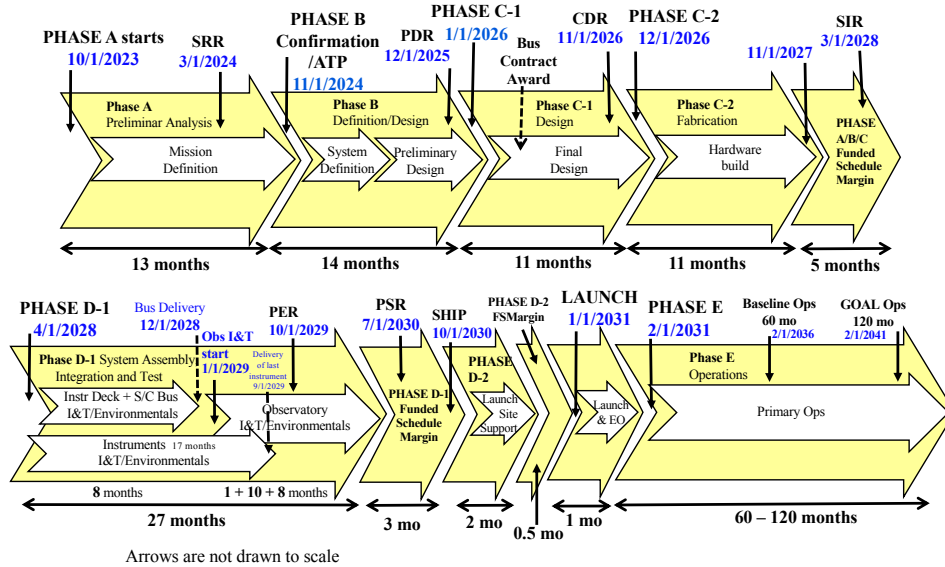

Figure 5: Top-level *STROBE-X* schedule developed in the MDL study.

6   Schedule

For the mission schedule, we followed the NASA guidance for probe-class missions being proposed to the 2020 Decadal Survey and used a Phase A start date of 2023 October 1.

Working with the GSFC IDL and MDL, we incorporated instrument construction, integration and test schedules based on our experience with *NICER* and *LOFT* to build a full mission schedule. This includes 8 months of funded schedule reserve, yielding an estimated launch date of 2031 January 1. We plan for a five-year prime mission. The schedule is presented in Fig. 5.

7 Cost Estimates

To be considered as a candidate probe-class mission, NASA requires that the total lifecycle mission cost estimate (Phases A–F) be less than $1B in FY 2018 dollars. NASA has provided guidance that: (1) $150M should be held for launch costs, (2) unencumbered cost reserves should be 25% of Phases A/B/C/D costs, (3) cost assumptions should be for un-modified Class B missions, (4) we should assume a Phase A start date of 2023 October 1.

The IDL and MDL studies provided detailed cost estimates for the instruments, spacecraft bus, ground systems, integration and test, and downlink costs, using a combination of parametric and grass roots costing. To that, we have added standard percentage "wraps" for WBS items like Project Management, Systems Engineering, Safety and Mission Assurance, Science, and Education and Public Outreach. For mission operations, we found that the wrap was

Astro2020 Probe Mission Preparatory Study
Master Equipment List Based Parametric Total Lifecycle Cost Estimate

Mission Name: **STROBE-X**
Cost Estimator: GSFC Code 158 (MDL and IDL)
Date of Cost Estimate: June 2018
Cost Estimate Based on: Final Master Equipment List

Project Phase	WBS Component	Cost (FY18 $M)	
Phase A	**Phase A Study**		**20**
Phases B–D	Mgmt, SE, MA	76	
	Science (incl. EPO)	12	
	XRCA	75	
	LAD	79	
	WFM	39	
	Spacecraft, incl. ATLO	172	
	System I&T	21	
	MOS/GDS	12	
	Launch Vehicle & Services	150	
	Reserves	112	
	TOTAL Phase B–D		**748**
Phases E–F	Science	30	
	Operations	83	
	Reserves	17	
	TOTAL Phases E–F		**130**
	TOTAL Lifecycle Cost		**898**

Figure 6: Top level mission cost estimate for the design developed in the GSFC IDL and MDL studies.

a significant underestimate compared to NASA guidance and historical precedent from missions like *Fermi*, so we increased it to $15M/year for the prime mission. Also, in response to feedback from the NASA Probes Cost Assessment Team (PCAT) we have increased our Phase A cost from what was in our Study Report. This process resulted in a total cost estimate comfortably below the probe class cost cap, with over 10% margin (*in addition to* the mandated 25% reserves), giving us very high confidence that this mission can be executed as a probe. We note that this cost estimate is very conservative in that it assumes all costs are borne by NASA. In reality, there would likely be a significant contribution from Europe that would reduce the cost to NASA (this could include detectors, instrument modules, an equatorial launch, for example).

In addition, the high degree of modularity in the design has many benefits that result in cost savings, improved reliability, and a straightforward descope path, if required.

As another demonstration of feasibility, we note that the last NASA Astrophysics mission in the probe class was *Fermi*, which has been operating highly successfully on orbit for a decade. *Fermi* had a total wet mass of 4400 kg and a total cost of $800M in FY17 dollars. The *Fermi*/LAT instrumented and read out 80 m^2 of silicon strip detectors, and the mission included an all-sky instrument, the GBM, which triggers autonomous repointing for transient events. So, in mass, electronic complexity and onboard processing, the success of *Fermi* supports our finding that *STROBE-X* can be executed as a probe-class mission.

References

[1] Aalto, S., et al. 2019, in BAAS, Vol. 51, 515

[2] Antoniou, V., et al. 2019, arXiv e-prints, arXiv:1901.01237

[3] Balsamo, E., et al. 2012, Proc. SPIE, 8450, 845052

[4] Bogdanov, S., et al. 2019, in BAAS, Vol. 51, 506

[5] Brandt, S., Hernanz, M., et al. 2014, Proc. SPIE, 9144, 2

[6] Brightman, M., et al. 2019, in BAAS, Vol. 51, 352

[7] Caiazzo, I., et al. 2019, in BAAS, Vol. 51, 516

[8] Civano, F., et al. 2019, in BAAS, Vol. 51, 429

[9] Cordes, J., McLaughlin, M. A., & Nanograv Collaboration. 2019, in BAAS, Vol. 51, 447

[10] Davis, S. W., Done, C., & Blaes, O. M. 2006, ApJ, 647, 525

[11] Drake, S. A., et al. 2015, ArXiv e-prints, 1501.02771

[12] Feroci, M., et al. 2012, Experimental Astronomy, 34, 415

[13] Fonseca, E., Demorest, P., Ransom, S., & Stairs, I. 2019, in BAAS, Vol. 51, 425

[14] Fryer, C., Burns, E., Roming, P., Couch, S., Szczepańczyk, M., Slane, P., Tamborra, I., & Trappitsch, R. 2019, in BAAS, Vol. 51, 122

[15] Garcia, J., et al. 2019, in BAAS, Vol. 51, 284

[16] Gatti, E., & Rehak, P. 1984, Nucl. Instrum. Meth. Phys. Res., 225, 608

[17] Gendreau, K. C., Arzoumanian, Z., et al. 2016, Proc. SPIE, 9905, 99051H

[18] Ginsburg, A., Mills, E. A. C., Battersby, C. D., Longmore, S. N., & Kruijssen, J. M. D. 2019, in BAAS, Vol. 51, 220

[19] Grin, D., Amin, M. A., Gluscevic, V., Hlozek, R., Marsh, D. J. E., Poulin, V., Prescod-Weinstein, C., & Smith, T. 2019, in BAAS, Vol. 51, 567

[20] Hebeler, K., Lattimer, J. M., Pethick, C. J., & Schwenk, A. 2013, ApJ, 773, 11

[21] Kalogera, V., et al. 2019, in BAAS, Vol. 51, 239

[22] Kamraj, N., Fabian, A., Lohfink, A., Baloković, M., Ricci, C., & Madsen, K. 2019, in BAAS, Vol. 51, 126

[23] Kara, E., et al. 2019, in BAAS, Vol. 51, 112

[24] Kelley, L., et al. 2019, in BAAS, Vol. 51, 490

[25] Kramer, M., & Wex, N. 2009, Classical and Quantum Gravity, 26, 073001

[26] Kupfer, T., Kilic, M., Maccarone, T., Burns, E., Fryer, C. L., & Wilson-Hodge, C. A. 2019, in BAAS, Vol. 51, 188

[27] Lattimer, J. M., & Prakash, M. 2001, ApJ, 550, 426

[28] Lazio, J., et al. 2019, in BAAS, Vol. 51, 135

[29] Maccarone, T., et al. 2019, in BAAS, Vol. 51, 186

[30] Maccarone, T., et al. 2019, in BAAS, Vol. 51, 226

[31] McHardy, I. M., Koerding, E., Knigge, C., Uttley, P., & Fender, R. P. 2006, Nature, 444, 730

[32] National Research Council. 2013, Nuclear Physics: Exploring the Heart of Matter (Washington, DC: The National Academies Press)

[33] Okajima, T., et al. 2016, Proc. SPIE, 9905, 99054X

[34] Osten, R., et al. 2019, in BAAS, Vol. 51, 393

[35] Rachevski, A., et al. 2014, Journal of Instrumentation, 9, P07014

[36] Ray, P. S., et al. 2018, in Society of Photo-Optical Instrumentation Engineers (SPIE) Conference Series, Vol. 10699, Proc. SPIE, 1069919

[37] Ray, P. S., et al. 2019, arXiv e-prints, arXiv:1903.03035, STROBE-X Study Report

[38] Read, J. S., Markakis, C., Shibata, M., Uryū, K., Creighton, J. D. E., & Friedman, J. L. 2009, Phys. Rev. D, 79, 124033

[39] Santander, M., et al. 2019, in BAAS, Vol. 51, 228

[40] Shafee, R., McClintock, J. E., Narayan, R., Davis, S. W., Li, L.-X., & Remillard, R. A. 2006, ApJL, 636, L113

[41] Shoemaker, D., & LIGO Scientific Collaboration. 2019, in BAAS, Vol. 51, 452

[42] Steiner, J. F., et al. 2019, in BAAS, Vol. 51, 359

[43] Uttley, P., Cackett, E. M., Fabian, A. C., Kara, E., & Wilkins, D. R. 2014, A&A Rv, 22, 72

[44] Uttley, P., Wilkinson, T., Cassatella, P., Wilms, J., Pottschmidt, K., Hanke, M., & Böck, M. 2011, MNRAS, 414, L60

[45] Uzdensky, D., et al. 2019, in BAAS, Vol. 51, 362

[46] Vacchi, A., et al. 1991, Nuclear Instruments and Methods A, 306

[47] Vitale, S., Gerosa, D., Haster, C.-J., Chatziioannou, K., & Zimmerman, A. 2017, Physical Review Letters, 119, 251103

[48] Wolff, M., et al. 2019, in BAAS, Vol. 51, 386

[49] Zane, S., et al. 2014, in Proc. SPIE, Vol. 9144, Space Telescopes and Instrumentation 2014: Ultraviolet to Gamma Ray, 91442W

[50] Zingale, M., Fryer, C., Hungerford, A., Safi-Harb, S., Trappitsch, R., Fisher, R., Calder, A., & Shen, K. 2019, in BAAS, Vol. 51, 259

[51] Zoghbi, A., et al. 2019, in BAAS, Vol. 51, 62